Phosphine Dissociation and Diffusion on Si(001) Observed at the Atomic Scale

Steven R. Schofield,* Neil J. Curson, Oliver Warschkow, Nigel A. Marks, Hugh F. Wilson, Michelle Y. Simmons, Phillip V. Smith, Marian W. Radny, David R. McKenzie, and Robert G. Clark

Centre for Quantum Computer Technology, School of Physics, University of New South Wales, Sydney 2052, Australia, School of Physics, University of Sydney, Sydney 2006, Australia, and the School of Mathematical and Physical Sciences, University of Newcastle, Callaghan 2308, Australia

Received: August 17, 2005; In Final Form: December 21, 2005

A detailed atomic-resolution scanning tunneling microscopy (STM) and density functional theory study of the adsorption, dissociation, and surface diffusion of phosphine (PH_3) on Si(001) is presented. Adsorbate coverages from ~0.01 monolayer to saturation are investigated, and adsorption is performed at room temperature and 120 K. It is shown that PH_3 dissociates upon adsorption to Si(001) at room temperature to produce both PH_2 + H and PH + 2H. These appear in atomic-resolution STM images as features asymmetric-about and centered-upon the dimer rows, respectively. The ratio of PH_2 to PH is a function of both dose rate and temperature, and the dissociation of PH_2 to PH occurs on a time scale of minutes at room temperature. Time-resolved in situ STM observations of these adsorbates show the surface diffusion of PH_2 adsorbates (mediated by its lone pair electrons) and the dissociation of PH_2 to PH. The surface diffusion of PH_2 results in the formation of hemihydride dimers on low-dosed Si(001) surfaces and the ordering of PH molecules along dimer rows at saturation coverages. The observations presented here have important implications for the fabrication of atomic-scale P dopant structures in Si, and the methodology is applicable to other emerging areas of nanotechnology, such as molecular electronics, where unambiguous molecular identification using STM is necessary.

1. Introduction

The ability to controllably position P dopant atoms into Si at the nanoscale is currently being developed by several groups because of the potential for creating nanoelectronic devices such as silicon single-electron transistors and quantum cellular automata.[1,2] This becomes particularly interesting when the control is extended to the level of positioning *individual* P dopant atoms,[3] which leads to the possibility of creating novel devices such as a single-dopant transistor[4] or even a silicon-based quantum computer.[5−7]

One promising method for achieving such atomic-scale control over the position of individual P atoms in Si is by controlling the chemical reaction of phosphine (PH_3) molecules with the Si(001) surface by using scanning tunneling microscopy (STM).[1,3,8] The interaction of PH_3 with the Si(001) surface has been the subject of numerous publications over the last two decades, using a variety of surface science techniques such as high-resolution electron energy loss spectroscopy[9] (HREELS), temperature programmed desorption[9,10] (TPD), Fourier transform infrared spectroscopy[11,12] (FTIR), X-ray photoelectron spectroscopy[13,14] (XPS), density functional theory calculations[11,15−18] (DFT), and scanning tunneling microscopy (STM).[12,13,19,18] In one of the earliest studies, Colaianni et al.[9] used HREELS and TPD to show that PH_3 adsorbs *dissociatively* at room temperature with no evidence for molecularly adsorbed PH_3. Subsequent FTIR and XPS measurements conclusively demonstrated that there are at least two major adsorbate species on Si(001) after exposure to PH_3 gas and that the relative concentration of these two species varies as a function of PH_3 dosing rate and substrate temperature.[11−14] Despite the earlier report of dissociative adsorption by Colaianni et al.,[9] Shan and co-workers[11,12] interpreted their FTIR data as evidence for both PH_3 and PH_2 adsorbates, and this interpretation was adopted by Lin and co-workers in their XPS study.[13,14] Atomic-resolution STM studies by three separate groups[12,13,19,18] did little to clarify the adsorption process. These studies reported that PH_3 adsorption to Si(001) results in primarily a single adsorbate species that appears in STM images as a circular (sometimes slightly elongated) protrusion located symmetrically above the Si dimers.[12,13,19,18] This adsorbate was respectively assigned to molecularly adsorbed PH_3,[12,19] dimer-inserted PH_2,[13] and surface P−P ad-dimers.[18] However, the possibility of this adsorbate being PH_3 was conclusively ruled out by DFT calculations performed by several different groups,[11,15−18] which showed that PH_3 could only adsorb to Si(001) in the dangling-bond position, and even then was unstable with respect to dissociation to PH_2. In addition, both dimer-inserted PH_2 and surface P−P are unlikely due to energetic barrier considerations. A less abundant feature seen in the STM images (that is also symmetric about the dimer rows) was assigned to etched Si monomers[12,19] or PH_x (x = 1, 2, 3) adsorbed at defect sites,[18] and has since been confirmed to be etched Si in the form of ad-dimers,[20] similar to the initial assignment of etched Si monomers by Wang et al.[19]

In an attempt to clarify the adsorption of PH_3 to Si(001) and, in particular, to understand STM images of this surface, we have embarked on an extensive investigation of this system by combining atomic-resolution STM measurements and DFT calculations. We have recently reported that the centered,

* Corresponding author. E-mail: steven.schofield@newcastle.edu.au.

10.1021/jp054646v CCC: $33.50
Published on Web 02/03/2006

circular adsorbate seen in previous STM studies is PH bonded in a bridge-site position above a Si dimer, with the two dissociated H atoms adsorbed to the adjacent Si dimer.[21,22] We have also reported the identification of several additional PH_3-related adsorbate species in STM images,[21,22] by far the most common of which produces a feature that is *asymmetric* about the dimer rows in STM images and which we believe is PH_2 and H bonded to opposite sides of a single Si dimer.

Our previous reports[21,22] have presented detailed DFT calculations of the adsorption and dissociation of PH_3 on Si(001), including total energy as well as barrier calculations, and discussed the expected surface features based on both *thermodynamic* and *kinetic* reaction considerations. Here, we present the direct experimental observation of PH_2 dissociation and diffusion on Si(001) in a detailed experimental atomic-resolution STM study. In particular, we conclusively demonstrate that the PH + 2H feature (centered protrusion) results from the surface dissociation of PH_2 from the PH_2 + H feature (asymmetric protrusion) to PH and a monohydride dimer. This dissociation process takes place on a time scale of minutes (in agreement with FTIR and XPS data[11−14]), and so the relative concentration of PH_2 and PH on saturation-dosed surfaces can be controlled by varying the dose rate. We show that the dissociation of PH_2 to PH does not occur at low temperature (120 K), but begins to occur upon warming the substrate to 200 K, in qualitative agreement with an Arrhenius temperature dependence. In addition, we show that at low surface-coverage PH_2 is able to diffuse on the Si(001) surface parallel to the dimer rows. This diffusion is closely related to the mechanism by which PH_2 dissociates to PH. We show that the surface diffusion of PH_2 is responsible for the formation of isolated hemihydride dimers on Si(001) after PH_3 dosing; this hemihydride dimer formation was previously a mystery, as it is known that H atoms do not surface diffuse on Si(001) at room temperature.[23] Finally, we show that the kinetics of PH_2 diffusion is responsible for the formation of ordered regions of PH + 2H molecules on Si(001) at high surface coverage.

The in situ experimental observations presented here are in excellent agreement with extensive DFT calculations[21,22] and together present a coherent picture for a complete mechanism of PH_3 adsorption and subsequent dissociation and diffusion on Si(001). This picture also fits well with the available data in the literature, with the slight concession that the interpretation of PH_3 and PH_2 adsorbates in a small number of publications should be reinterpreted as PH_2 and PH, and we discuss good reasons for doing this at the end of the paper.

2. Experimental Section

Experiments were performed by using an Omicron variable temperature STM inside an ultrahigh vacuum (UHV) chamber with base pressure $<5 \times 10^{-11}$ mbar. Phosphorus-doped 10^{15} cm^{-3} wafers, orientated toward the [001] direction, were used. All Si samples were handled only by using ceramic tweezers and mounted in tantalum/molybdenum/ceramic sample holders to avoid contamination. Sample preparation was performed by outgassing overnight at 850 K, followed by oxide removal at 1400 K and cooling slowly (~3 K/s) from 1150 K to room temperature.[24] PH_3 is a dangerous gas, being both highly toxic and flammable, and so special care was taken in its use in our laboratory: less than one cubic centimeter of ultrapure PH_3 gas at atmospheric pressure was housed in a leak-monitored double-walled containment system. PH_3 was admitted to the STM chamber via a leak valve with line-of-sight to the sample while mounted in the STM. Care was taken to ensure no hot filaments were close by or in line-of-sight to the sample during PH_3 dosing to ensure that the PH_3 was not dissociated before reaching the sample surface.

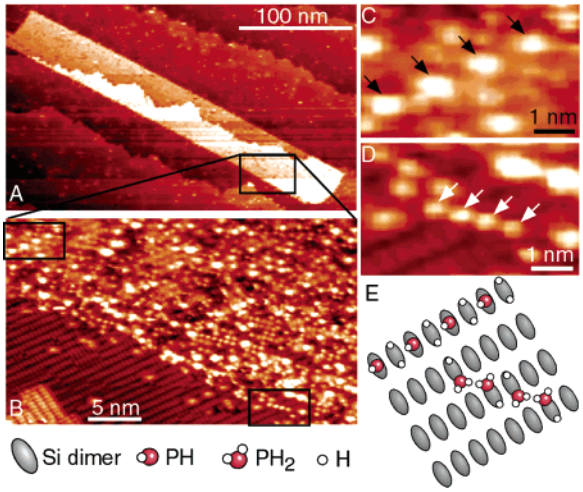

Figure 1. (A) 300 × 50 nm^2 lithographic patch of bare Si(001) surface surrounded by H-terminated Si(001). (B) Enlargement of the boxed region in (A) after exposure of the substrate to 0.14 L of PH_3. (C) Enlargement from top left boxed region of (B) showing four PH + 2H adsorbates in a line. (D) Enlargement from bottom right boxed region of (B) showing four collinear PH_2 + H adsorbates. (E) Schematic showing the bonding arrangements of the molecules shown in (C, D). All images: −2.0 V sample bias, 0.2 nA tunneling current.

3. Saturation-Dosed Surfaces

A useful way to observe the bonding arrangements of molecules on Si(001) is to limit the spatial extent of the adsorption to only a small area by using hydrogen lithography.[25,26] This is achieved by terminating the surface with a monolayer of hydrogen and subsequently removing the H from a small region by performing electron stimulated desorption using the highly confined electron beam of the STM tip. An example of this is shown in Figure 1A, where a ~300 × 50 nm^2 rectangular patch of bare Si(001) surface has been exposed on an otherwise H-terminated Si(001) surface (details of the H termination and H lithography steps have been presented previously[3]). The patch of bare Si(001) surface appears brighter in the STM image due to the additional STM tunneling current that arises from the Si surface π-states.[27] The surface shown in Figure 1A was subsequently exposed to 0.14 L of PH_3 at a chamber pressure of 1×10^{-9} mbar, and a small section of the PH_3 dosed surface is shown in Figure 1B. The PH_3 molecules are not able to adsorb on the chemically passivated areas of H-terminated surface that surround this patch, which can therefore be used as a reference where the (2 × 1) dimer periodicity of the Si(001) surface can be observed. This allows the identification of the bonding sites and surface ordering of the adsorbates within the patch with respect to the Si(001) surface.

Both the PH + 2H and PH_2 + H features are seen within the lithographic patch in Figure 1B. Four of the PH + 2H features are shown in Figure 1C, which is an enlargement of the top left corner of Figure 1B. These molecules are adsorbed on every other dimer along the dimer row, consistent with first principles calculations that predict the formation of a monohydride dimer adjacent to the PH molecule.[21,22] Figure 1D shows an enlargement of the bottom right corner of Figure 1B, where four of the PH_2 + H features can be observed. We see from Figure 1B and D that these molecules self-order on the surface

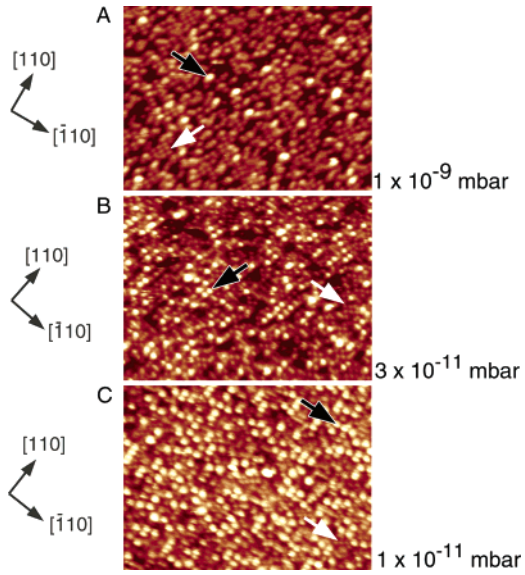

Figure 2. Si(001) surfaces dosed to saturation with PH_3 with varying dose rates. The dose rates were monitored by measuring the increase in total chamber pressure during PH_3 dosing, which were (A) 10^{-9} mbar; (B) 3×10^{-11} mbar; and (C) 1×10^{-11} mbar. To reach saturation coverage, the dose time varied from 10 min for (A), 100 minutes for (B), and 5 h for (C). White arrows indicate $PH_2 + H$ features, while black arrows indicate $PH + 2H$ features. Each image is 30×25 nm^2 in area. All images were acquired with ~ -3 V sample bias and $\sim$0.2 nA tunneling current.

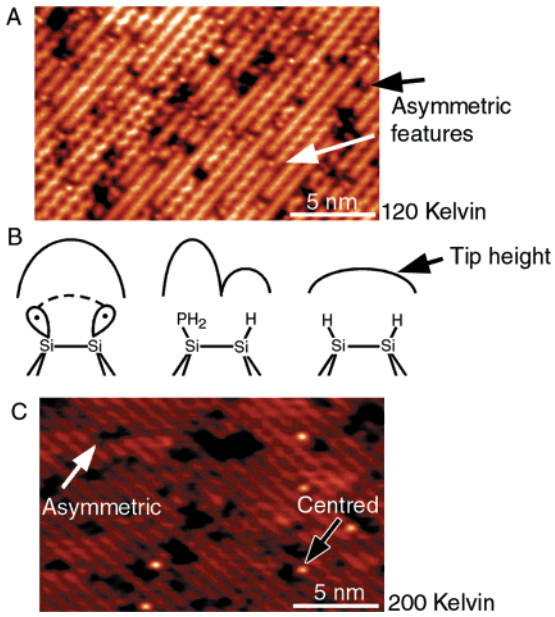

Figure 3. PH_3 adsorption on Si(001) at cryogenic temperatures. (A) Si(001) cooled to 120 K and exposed to a PH_3 partial pressure of 3×10^{-11} mbar for 6 min. No $PH + 2H$ adsorbates were observed after dosing at 120 K. (B) Schematic diagram to highlight the apparent height difference of a PH_2 molecule when imaged on a clean Si(001) surface and a H-terminated Si(001) surface. (C) This surface was prepared in the same manner as the surface shown in (A) and then allowed to warm slightly to 200 K. Parameters for both images: -4.5 V, 0.4 nA.

with a $p(2 \times 2)$ periodicity. The schematic shown in Figure 1E shows the bonding locations and ordering for the four $PH + 2H$ and four $PH_2 + H$ features shown in Figure 1C and D, respectively. The majority of features within the lithographic patch can be attributed to $PH_2 + H$ or $PH + 2H$ features; however, a small number of depression and protrusion features can be attributed to isolated H atoms and Si dangling bonds. The observation of these adsorbates and, in particular, their self-ordering on the surface, confirms these as the primary PH_x ($x = 1, 2$) moieties formed after dosing the Si(001) surface to saturation coverage at room temperature.

Changes in the ratio of PH_2 to PH are observed to occur during the course of an STM experiment. This suggests that the dissociation from PH_2 to PH may take place on a time scale of minutes. If this is so, a sample that is dosed very slowly, i.e., over a period of some hours, should exhibit an elevated number of $PH + 2H$ features compared to that of a surface dosed to saturation more quickly, and we have found that this is indeed the case. Figure 2A shows a surface dosed to saturation in $\sim$10 min by filling the chamber to a pressure of 1×10^{-9} mbar. This surface has a high number of $PH_2 + H$ features and patches of these molecules ordering with $p(2 \times 2)$ periodicity can be seen, as highlighted by the white arrow.

The surface shown in Figure 2B was formed by dosing with a 3×10^{-11} mbar partial pressure of PH_3 and dosing for 100 minutes. As expected, the number of $PH + 2H$ features has increased compared to that of the surface in Figure 2A. In addition, we see a tendency for the PH molecules to line up along a dimer row (due to the anisotropic diffusion of PH_2 that we will discuss below), and in all cases, the centered protrusions are separated by at least one dimer width. Nevertheless, small patches of PH_2 features with $p(2 \times 2)$ periodicity can be observed on this surface. Finally, we have dosed a Si(001) sample at the slowest rate possible in our instrument by dosing the sample for 5 h with the total chamber pressure raised by just 1×10^{-11} mbar above background pressure. The resulting surface, shown in Figure 2C, exhibits an even greater proportion of $PH + 2H$ features (over 200 in Figure 2C compared with $\sim$150 in Figure 2B), with only a few small regions of $PH_2 + H$ observable in the image (Note that in each case these images are representative of the entire surface of the sample). Figure 2 represents direct experimental evidence that the $PH + 2H$ feature (centered protrusion) is the dissociation product of PH_2 from the $PH_2 + H$ feature (asymmetric protrusion). Furthermore, these images unambiguously demonstrate that this dissociation takes place on a time scale of minutes at room temperature and occurs regardless of whether the surface is imaged with the STM or not.

4. Adsorption at Low Temperature

The dissociation of PH_3 on Si(001) is an activated process that is expected to follow an Arrhenius dependence on temperature. Therefore, the dissociation should be inhibited when the sample is cooled to cryogenic temperatures. Figure 3 shows the results of two experiments where the PH_3 dosing and STM imaging were performed at cryogenic temperature by coupling the sample to a liquid nitrogen cryostat. The sample temperature was monitored by a silicon diode coupled to the sample holder. The surface shown in Figure 3A was cooled to $\sim$120 K and then exposed to 0.008 L of PH_3 at a chamber pressure of 3×10^{-11} mbar. This surface exhibits a uniform coverage of $PH_2 + H$ features, but has a complete absence of any $PH + 2H$ features.[28] The surface shown in Figure 3A was imaged continuously for several hours with no observation of $PH + 2H$ features. We have also dosed Si(001) samples to saturation coverage with PH_3 at 120 K (not shown) and, again, find no evidence for any $PH + 2H$ features. The absence of $PH + 2H$ features is consistent with the dissociation of PH_2 to PH being inhibited at 120 K and further confirms our assignment of the centered feature to PH molecules resulting from the dissociation of PH_2 on the surface.

A closer inspection of Figure 3A reveals that there appear to be two distinct types of asymmetric features, as indicated by the white and black arrows, respectively. This second asymmetric protrusion can reasonably be attributed to molecularly adsorbed PH_3 molecules because the dissociation of PH_3 to PH_2 may be inhibited at 120 K to the point where some undissociated PH_3 remains on the surface.

Alternatively, these features may be attributed to a different configuration of PH_2, for example, one in which the dimer end opposite to the PH_2 is not terminated with a H atom. We will discuss further below how such structures may come about. Further low-temperature experiments are underway to rule out one or another of the above possibilities and identify the second asymmetric protrusion seen at 120 K as either undissociated PH_3 or an alternate configuration of PH_2.

Figure 3C shows a Si(001) surface exposed to PH_3 at 120 K and then allowed to warm slightly to 200 K. In this image, several PH + 2H features can be seen, indicating that some dissociation of PH_2 to PH occurs at this temperature. The relatively low coverage of PH + 2H features in Figure 3C compared to that of a surface exposed to an equal fluence of PH_3 at room temperature is consistent with an Arrhenius temperature dependence for PH_2 dissociation.

5. Quantum Chemistry Calculations

To further understand the dissociation processes leading from molecularly adsorbed PH_3 to PH_2 + H and PH + 2H species, we have conducted quantum chemical calculations of the energetics of these species and explored probable reaction pathways and transition barriers. The objective of these calculations is to provide an overview of the activation energies that govern the observed transitions. We present here only the key aspects of our theoretical results relating to the observed transitions, and refer the reader to the full details to be published elsewhere. Briefly, our calculations were conducted at the B3LYP/6-311++G(d,p) level of density functional theory (DFT) by using a three-dimer $Si_{21}H_{20}$ cluster model of the Si(001) surface. We note that this type of cluster model has been used variously in the literature to describe reactions on the Si(001) surface and has been found to give adequate reaction energies.[29] In our calculations, all atomic positions are fully relaxed with the exception of the cluster terminating H atoms, which are locked into position along truncated Si−Si bonds so as to mimic the strain imposed on the cluster by the surrounding crystal. We note further that, for computational efficiency, the atomic basis set is truncated for second-layer Si atoms to the 6-311G(d) level and for third- and fourth-layer Si atoms as well as the cluster-terminating H atoms to the LANL2DZ level. All calculations were conducted using the Gaussian 03 software.[30]

An overview of our computational results is shown in Figure 4. For clarity and consistency, we adopt the nomenclature of ref 22 (Warschkow et al., 2005) where PH_x + (3 − x)H structures with $x = 3$, 2, and 1 are designated by using the letters A, B, and C, respectively, and different bonding geometries are sequentially numbered. In particular, we designate molecularly adsorbed PH_3 as structure A1, three different configurations of PH_2 + H as structures B1, B2, and B4,[31] and PH + 2H as structure C1 (see Figure 4A).

A schematic of two reaction pathways from adsorbed PH_3 to PH + 2H (A1 → B1 → B4 → C1 and A1 → B2 → B4 → C1) is shown in Figure 4A. The corresponding energetics of the intermediate structures and transition states are shown in Figure 4B. The dissociation of molecularly adsorbed PH_3 (A1) to PH_2 + H, with both fragments attached to opposite ends of the same dimer (B1), has been described previously by Miotto et al.[15] In

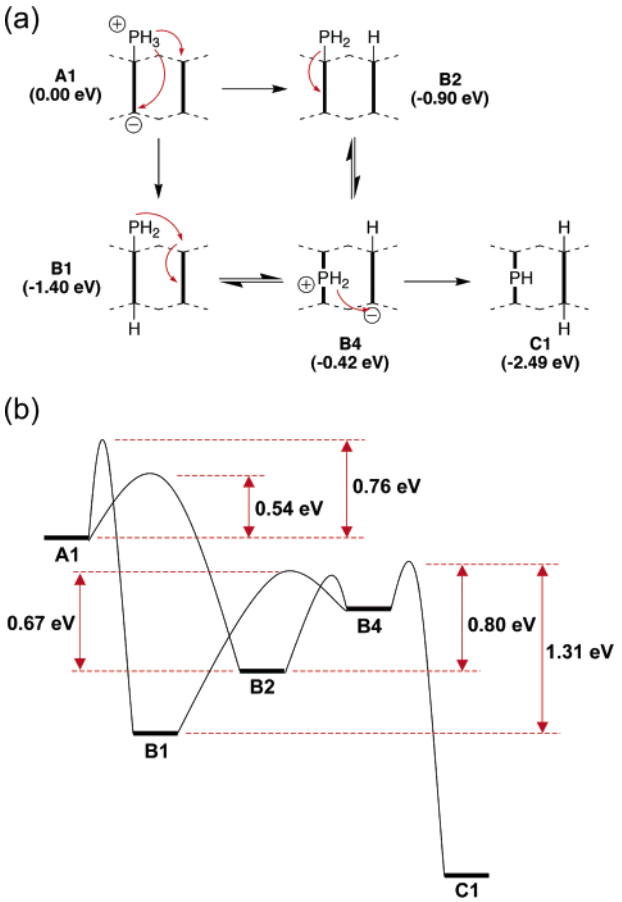

Figure 4. Schematic reaction mechanism (A) and energy diagram (B) of the dissociation of molecularly adsorbed PH_3 to PH_2 + H and PH + 2H species as calculated by density functional theory. The focus of the energy diagram in (B) is on the principal intermediates and the governing transition states between them. For simplification, a number of minor intermediates not relevant to this discussion have been omitted.

qualitative agreement with these calculations,[15] we find that the formation of B1 leads to a substantial stabilization of 1.40 eV and is accessible with a relatively low activation energy of 0.76 eV (Figure 4B). An alternative dissociation channel is one that leads to structure B2 (Figure 4A) via a proton-shift reaction to an adjacent dimer in a manner analogous to that reported for NH_3 dissociation on Si(001) by Smedarchina et al.[32] The activation barrier for the dissociation from PH_3 (A1) to structure B2 is 0.54 eV, which is 0.22 eV lower than the barrier for dissociation from PH_3 to structure B1. Thus, B2 is the *kinetically favored* product, and we therefore expect some of the molecularly adsorbed PH_3 to dissociate via the B2 structure. Structure B1, however, is 0.50 eV more stable than B2 and is therefore the *thermodynamically favored* product.

We now consider the further dissociation of products B1 and B2 toward the PH + 2H feature, C1. In structure C1, PH is centered on top of a Si−Si dimer, forming a three-membered ring, and the two hydrogen atoms are attached to a neighboring dimer in the same row. We identify structure B4 as the most likely, if highly transient, precursor to C1. As shown in Figure 4, the B4 structure contains a dimer centered PH_2 and a H atom on the adjacent dimer. Both the B1−B4 and B2−B4 reactions are endothermic. B4 is 0.98 eV less stable than B1 and 0.48 eV less stable than B2, which makes B4 a very short-lived (transient) intermediate; once formed, it will either quickly convert to the much more stable PH + 2H structure C1 (irreversible) or else convert back to one of the PH_2 + H structures B1 and B2.

Structure B4 is reached from structure B2 by a one-step reaction in which the lone pair on the phosphorus extends to the free Si atom on the other dimer end. This leads to the formation of a second bond between P and Si, which closes the three-membered ring. The path from B1 to B4 is more complicated and involves several steps; principally, a shift of the PH_2 group from one Si−Si dimer end to the next, followed by a ring-closure reaction to form structure B4 with PH_2 in the dimer-center position. It is the second step, the ring-closure, that has the highest energy and is therefore the rate-determining transition state in the formation of B4.

From the calculated transition barriers, the (classical) rate of dissociation can be estimated via an Arrhenius ansatz and a typical attempt frequency of 10^{14} s^{-1}.[33] This yields a room-temperature lifetime below 0.1 s for the dissociation of molecularly adsorbed PH_3 (structure A1) to both PH_2 + H structures B1 and B2 (the barriers are 0.76 and 0.54 eV, respectively). This is consistent with the nonobservation of undissociated PH_3 on Si(001) at room temperature in our STM measurements.

The lifetime of the thermodynamically favored PH_2 + H structure B1 (the asymmetric feature in STM images) is dependent on the highest transition point along a low-energy reaction path, leading to the more stable PH + 2H structure C1. This highest transition point (given by the B4−C1 reaction step) yields an effective barrier of 1.31 eV, which B1 has to surmount before it can stabilize to C1. Thus, the reaction of the B1 PH_2 + H structure to the PH + 2H feature C1 will occur much more slowly than the dissociation of molecularly adsorbed PH_3 to PH_2 + H. This is in good qualitative agreement with our STM observation of a mixture of PH_2 + H and PH + 2H on Si(001) at room temperature and a complete absence of any undissociated PH_3. We note that the calculated barrier height of 1.31 eV for the B1−C1 transition is slightly too high for the experimentally observed rate of the order of minutes (suggesting a barrier of ∼1.1 eV); however, this is within the expected errors associated with making quantitative predictions from such calculations.[33] In particular, we note that the crucial B4−C1 transition is a proton-shift reaction and that consideration of quantum tunneling effects can lead to a substantial enhancement of the expected rate of such reactions.[32] The kinetically favored PH_2 + H structure B2 can stabilize to either the PH_2 + H (asymmetric feature; structure B1) or to PH + 2H (centered feature; structure C1) with effective barriers of 0.67 and 0.80 eV, respectively. These barriers are only marginally higher than A1−B1/B2 transitions. Thus, while the B2 structure is the kinetically favored dissociation product of molecularly adsorbed PH_3 (A1), it dissociates to C1 or rearranges to B1 almost as rapidly as it is formed. This explains the absence of any features in our room-temperature STM experiments that are consistent with the B2 structure.

6. Surface Diffusion

We now turn our attention to imaging individual, isolated PH_x $\{x = 1, 2\}$ adsorbates at room temperature on lightly PH_3 dosed Si(001) surfaces and compare successive images of the same area to observe dissociation and/or diffusion events. To do this, it is necessary to observe a large enough area that both the initial and final positions of the molecule can be determined (the scan speed of the STM is much slower than the time it takes for individual events to occur). In most cases, on the Si(001) surface, it is sufficient to observe a region of surface bounded by two neighboring step edges. Figure 5 shows a series of filled-state STM images that have been cropped down from

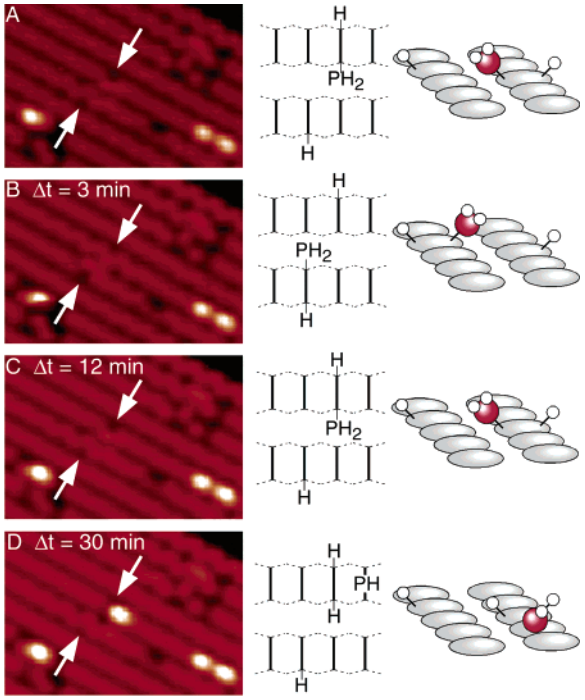

Figure 5. (A) PH_2 + H (top right arrow) and hemihydride dimer (bottom left arrow). (B) The PH_2 molecule seen in (A) has surface diffused to the site of the hemihydride dimer in (A). This diffusion results in the formation of a PH_2 + H feature at the bottom left arrow and leaves behind a hemihydride dimer at the top right arrow, giving the impression that the two features in (A) have swapped places. (C) The PH_2 molecule moves back to its initial position. (D) The PH_2 molecule dissociates to PH + 2H, and no further change in the bottom hemihydride is observed. These transitions are illustrated in both schematic and cartoon representation to the right of the STM images. All images are ∼9.5 × 5.5 nm^2 in area and were acquired with −2 V sample bias and 0.2 nA tunneling current.

larger (50 × 50 nm^2) images (not shown), where two such neighboring step edges are visible. In Figure 5A, we see a PH_2 + H feature (top right arrow), with a hemihydride dimer on the adjacent row (bottom left arrow).

The hemihydride dimer in this image exhibits the zigzag appearance known to be characteristic of these features in filled-state STM images.[34] The images shown in Figure 5B−D show the same area of the surface taken in subsequent scans with the STM; the scanning speed of the STM was such that one full image was acquired every 3 min. Careful observation of Figure 5B reveals that the asymmetric feature and the hemihydride dimers have apparently switched places. In fact, it is only the PH_2 molecule that moves; this molecule is able to diffuse down the dimer row toward the hemihydride in the adjacent row. At this point, the dangling bond of the hemihydride dimer on the neighboring dimer row presents a low-energy position and the PH_2 molecule jumps across the dimer row to occupy this position. The net result is that the hemihydride dimer in Figure 5A is effectively converted into an PH_2 + H feature, while the PH_2 + H feature in Figure 5A is converted to a hemihydride dimer. It should be noted that the conversion of these two features was the only event that occurred along the entire lengths of these two dimer rows between these two images, ruling out the possibility of other molecules on the surface taking part in the transition observed between Figure 5A and B.

The two features discussed in Figure 5B were unchanged in the subsequent two STM images. However, in the third image taken after Figure 5B, the PH_2 molecule has diffused back to its original position, as shown in Figure 5C. In 20 STM images

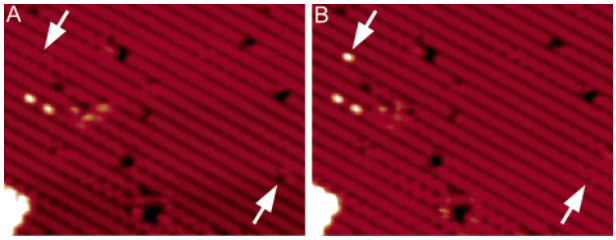

Figure 6. Diffusion of PH_2 on Si(001). (A) Lightly PH_3 dosed Si(001) surface. A hemihydride (upper left) and PH_2 + H (lower right) are indicated by arrows. (B) Same area as (A) acquired 3 min afterward. The PH_2 from at the lower right arrow in (A) has diffused along the dimer row to the upper left arrow where it has interacted with the hemihydride dimer and dissociated to PH + 2H. This diffusion leaves behind a hemihydride at the lower right arrow in (B). The overall process is analogous to that shown in Figure 5. Images are ~17 × 15 nm^2, acquired with −2 V sample bias and 0.2 nA tunneling current.

acquired over a period of 1 h, the PH_2 molecule was imaged in its rightmost position 13 times and in the leftmost position 7 times. The PH_2 molecule may have moved many more times than is indicated by these 20 images, as we effectively only observed its position once every three minutes. However, we can say that the two hemihydride dimers present low-energy sites for the PH_2 molecule to reside in with a reasonably low energetic barrier for diffusion and that the molecule was not observed to reside in any other position on the surface during the hour that we imaged it.

In Figure 5D, we have a departure from the diffusing of the PH_2 molecule from one location to the other; we now see a PH + 2H protrusion at the top right position and a hemihydride in the lower left position. The PH + 2H protrusion is accompanied by a one-dimer-wide depression on its left side, known to be characteristic of its appearance in filled-state STM images.[21] At some time between the images shown in Figure 5C and D, the PH_2 molecule has dissociated to PH as discussed in Section 5; i.e., the PH_2 molecule has shifted across to occupy a dimer-bridge position on the neighboring Si dimer and subsequently dissociated via a proton-shift reaction. The proton shift is back toward the adjacent hemihydride dimer, resulting in the formation of a monohydride dimer that appears dark in the STM image and produces the depression seen adjacent to the PH + 2H protrusion in Figure 5D.

The hemihydride dimer shown in Figure 5D remained unchanged for the next 70 min, during which it was imaged, in agreement with the energetic calculations presented in the previous section. The PH + 2H feature in Figure 5D further dissociated to a *U-shaped* P + 3H feature (not shown; we have described the spontaneous dissociation of PH to this U-shaped feature previously[21]) 5 min after the image shown in Figure 5D was acquired and remained in this state for the remainder of the time it was imaged, more than an hour.

Figure 6 shows a pair of images of a lightly PH_3 dosed Si(001) surface, where we see a diffusion and dissociation event similar to that shown in Figure 5. In this case, however, we see the diffusion of the PH_2 molecule to extend much farther along the dimer row (~15 nm) before dissociation. In Figure 6A, we see a PH_2 + H feature indicated by an arrow in the lower right of the image and a hemihydride dimer indicated by an arrow at the top left of the image. Figure 6B shows an image of the same surface area taken 3 min later. We see in this image that the PH_2 molecule has diffused along the dimer row toward the top left of the image. Upon reaching the site of the hemihydride dimer, the PH_2 molecule dissociates to PH + 2H in a manner analogous to that seen in Figure 5. Figures 5 and 6 show two examples of the surface diffusion and dissociation of PH_2 on Si(001) that has been observed routinely in our experiments.

It is worth pointing out that the mechanism by which PH_2 diffuses along the dimer row is closely related to the mechanism for the dissociation of PH_2 to PH. As we discussed in Section 5, the first stage of PH_2 dissociation (from the asymmetric B1 structure) involves a shift of the PH_2 molecule from the end of one Si dimer to the end of the adjacent dimer. This shift is facilitated by the lone pair orbital of the PH_2 molecule (note the PH_2 has a lone pair because it has a third bond to a Si atom on the surface), forming a dative bond with the nucleophilic site of the adjacent Si dimer. Diffusion of the PH_2 molecule along the row occurs when this shift is repeated for successive dimers along the dimer row. As shown in Figure 6, we have observed the anisotropic diffusion of PH_2 to occur over distances up to 15 nm before dissociating to PH at the site of an existing defect such as a hemihydride dimer or existing PH molecule. This leads us to speculate that the probability of the PH_2 molecule shifting into the B4 configuration (Figure 4A) and subsequently dissociating to PH + 2H (C1) is greatly enhanced by the presence of such defects in the dimer row. Thus, we believe that the formation of short chains of PH + 2H features on saturation-dosed surfaces (such as seen in Figure 2B) can be attributed to the anisotropic diffusion of PH_2.

The fact that it is the lone pair orbital of the PH_2 adsorbate that facilitates its anisotropic diffusion explains why we do not observe diffusion for species such as the PH + 2H adsorbate. However, by analogy, we expect that this diffusion mechanism will be important for other molecules adsorbed to Si(001) that have lone pair orbitals, such as AsH_2.

The data presented here are in good agreement with previous studies using alternative surface science techniques. Colaianni et al.[9] have shown that all PH_3 dissociates to PH_2 upon adsorption to Si(001) at room temperature and that all PH_2 is completely dissociated after annealing to ~375 °C, in excellent agreement with our results (we have reported the complete dissociation of PH_3 after annealing to ~350 °C in Ref 3). A subsequent key paper by Shan et al.[11] used FTIR to conclude that the adsorption of PH_3 to Si(001) was only partially dissociative at room temperature and the majority species was molecularly adsorbed PH_3. However, as we have discussed in detail in a previous report,[22] we believe the data in this paper can be reinterpreted in a sensible and straightforward way that makes it consistent with our results; essentially, the triplet group of infrared P−H stretch modes assigned to PH_3 by Shan et al.[11] should instead be assigned to PH_2. Vibrational frequency calculations[22] performed using the Gaussian package suggest that PH_3 will produce a single high-intensity peak with a doublet of smaller peaks, unlike the three peaks of similar intensity reported by Shan et al.[11] The same calculations suggest that PH_2 will produce four stretch modes (two each from two different conformations), but two of the peaks are closely spaced and might therefore be observed as a single peak. A more recent paper by Lin et al.[13] reports the appearance of two dominant adsorbate species in XPS data and assigns these to PH_3 and PH_2. However, no additional experimental evidence for assigning the adsorbates as PH_3 and PH_2 is presented by Lin et al.,[13] and when instead interpreted as PH_2 and PH, their data is in good agreement with the results we have presented here. Finally, our interpretation is in good agreement with all DFT calculations and STM measurements so far reported for this system[11−19] in contrast to the interpretation of partially dissociative adsorption, which is at odds with these reports.

We make two general comments on the study of adsorbates with STM: (1) The data we have presented reinforces the point that, when analyzing STM images of adsorbates on semiconductor surfaces, it is not sufficient to consider only features that appear as *protrusions* above the surface plane. We have shown that PH_2 molecules are imaged on the Si(001) surface with an apparent intensity that is equal to the surrounding silicon dimers. This is undoubtedly the reason that this molecule remained unidentified until it was imaged within lithographic patches on H-terminated Si(001) surfaces such as in Figure 1. (2) We note the importance of observing *transitions* between successive STM images in identifying adsorbates. By observing such transitions and carefully comparing the results with ab initio calculations, we have been able to identify the diffusion of PH_2 molecules on Si(001) and their subsequent dissociation.

In summary, we have performed a combined STM/DFT study of the adsorption of PH_3 to Si(001) at room temperature and 120 K. At room temperature, we find the adsorption is dissociative, producing both PH_2 and PH adsorbate species. PH_2 adsorbates are predominantly found as part of a $PH_2 + H$ structure where each fragment is bound to opposite ends of a single dimer, and this produces a feature that appears asymmetric about the dimer row in STM images. PH is generally found with the PH fragment bound in a dimer-bridge position about a single Si dimer and the two dissociated H atoms bound to an adjacent Si dimer. The appearance of this feature in filled-state STM images is a bright circular protrusion (PH) with an adjacent dimer-sized depression (H−Si−Si−H). The relative coverage of these two adsorbate species is dependent on the PH_3 dose rate because the dissociation of PH_2 to PH occurs on a time scale of minutes. At 120 K, the dissociation of PH_2 to PH is completely inhibited but begins to occur upon warming to 200 K. By studying low-coverage surfaces at room temperature, we have observed the in situ diffusion and dissociation of PH_2. DFT calculations show that this diffusion is facilitated by the lone pair orbital of the PH_2 adsorbate, and we therefore expect this mechanism to be important for other molecules bound to Si(001) that have lone pair orbitals. PH_2 is responsible for the formation of hemihydride dimers on the low PH_3 dosed Si(001) surface and the lining up of PH molecules along dimer rows on Si(001) surfaces at saturation coverages. The data we present here has important implications for the fabrication of atomic-scale P dopant structures in Si. In addition, the principles of molecular identification using STM that we have presented here will be of interest to researchers in related fields such as molecular electronics.

Acknowledgment. S.R.S. acknowledges an Australian Government Postdoctoral Fellowship, and both M.Y.S. and R.G.C. acknowledge Australian Government Federation Fellowships. This work was supported by the Australian Research Council, the Australian Government, the U.S. Advanced Research and Development Activity, U.S. National Security Agency, and U.S. Army Research Office under contract DAAD19-01-1-0653.

References and Notes

(1) Tucker, J. R.; Shen, T. C. *Int. J. Circ. Theor. Appl.* **2000**, *28*, 553−562.

(2) Anconaa, M. G. *J. Appl. Phys.* **1996**, *79*, 526.

(3) Schofield, S. R.; Curson, N. J.; Simmons, M. Y.; Ruess, F. J.; Hallam, T.; Oberbeck, L.; Clark, R. G. *Phys. Rev. Lett.* **2003**, *91*, 136104.

(4) Ono, Y.; Fujiwara, A.; Takahashi, Y.; Inokawa, H. *Mater. Res. Soc. Symp. Proc.* **2005**, *864*, E6.7.1.

(5) Kane, B. E. *Nature* **1998**, *393*, 133−137.

(6) Das Sarma, S.; de Sousa, R.; Hu, X.; Koiller, B. *Solid State Comm.* **2005**, *133*, 733.

(7) Schenkel, T.; Persaud, A.; Park, S. J.; Nilsson, J.; Bokor, J.; Liddle, J. A.; Keller, R.; Schneider, D. H.; Cheng, D. W.; Humphries, D. E. *J. Appl. Phys.* **2003**, *94*, 7017.

(8) Tucker, J. R.; Shen, T. C. *Solid-State Electron.* **1998**, *42*, 1061.

(9) Colaianni, M. L.; Chen, P. J.; Yates, J. T., Jr. *J. Vac. Sci. Technol., A* **1994**, *12*, 2995.

(10) Yoo, D. S.; Suemitsu, M.; Miyamoto, N. *J. Appl. Phys.* **1995**, *78*, 4988.

(11) Shan, J.; Wang, Y.; Hamers., R. J. *J. Phys. Chem.* **1996**, *100*, 4961.

(12) Hamers, R. J.; Wang, Y.; Shan, J. *Appl. Surf. Sci.* **1996**, *107*, 25−34.

(13) Lin, D. S.; Ku, T. S.; Sheu, T. J. *Surf. Sci.* **1999**, *424*, 7−18.

(14) Lin, D.-S.; Ku, T.-S.; Chen, R.-P. *Phys. Rev. B* **2000**, *61*, 2799.

(15) Miotto, R.; Srivastava, G. P.; Ferraz, A. C. *Phys. Rev. B* **2001**, *63*, 125321.

(16) Miotto, R.; Srivastava, G. P.; Ferraz, A. C. *Surf. Sci.* **2001**, *482−485*, 160−165.

(17) Cao, P.-L.; Lee, L.-Q.; Dai, J.-J.; Zhou, R.-H. *J. Phys.: Condens. Mater.* **1994**, *6*, 6103−6109.

(18) Kipp, L.; Bringans, R. D.; Biegelsen, D. K.; Northrup, J. E.; Garcia, A.; Swartz, L. E. *Phys. Rev. B* **1995**, *52*, 5843.

(19) Wang, Y.; Bronikowski, M. J.; Hamers, R. J. *J. Phys. Chem.* **1994**, *98*, 5966.

(20) Curson, N. J.; Schofield, S. R.; Simmons, M. Y.; Oberbeck, L.; O'Brien, J. L.; Clark, R. G. *Phys. Rev. B* **2004**, *69*, 195303.

(21) Wilson, H. F.; Warschkow, O.; Marks, N. A.; Schofield, S. R.; Curson, N. J.; Smith, P. V.; Radny, M. W.; McKenzie, D. R.; Simmons, M. Y. *Phys. Rev. Lett.* **2004**, *93*, 226102.

(22) Warschkow, O.; Marks, N.; Wilson, H. F.; Schofield, S. R.; Curson, N. J.; Smith, P. V.; Radny, M. W.; McKenzie, D. R.; Simmons, M. Y. *Phys. Rev. B* **2005**, *72*, 125328.

(23) Owen, J. H. G.; Bowler, D. R.; Goringe, C. M.; Miki, K.; Briggs, G. A. D. *Phys. Rev. B* **1996**, *54*, 13153.

(24) Swartzentruber, B. S.; Mo, Y. W.; Webb, M. B.; Lagally, M. G. *J. Vac. Sci. Technol., A* **1989**, *7*, 2901.

(25) Shen, T. C.; Wang, C.; Abeln, G. C.; Tucker, J. R.; Lyding, J. W.; Avouris, P.; Walkup, R. E. *Science* **1995**, *268*, 1590.

(26) Lyding, J. W.; Shen, T. C.; Hubacek, J. S.; Tucker, J. R.; Abeln, G. C. *Appl. Phys. Lett.* **1994**, *64*, 2010.

(27) Hamers, R. J.; Avouris, P.; Bozso, F. *Phys. Rev. Lett.* **1987**, *59*, 2071.

(28) We note that the asymmetric protrusions in Figure 3A appear at a similar intensity as the surrounding bare Si(001) surface plane, whereas those we saw in Figure 1B and D protruded above the surrounding H-terminated Si(001) surface plane. This is due to the apparent height increase of the clean Si(001) surface over the H-terminated Si(001) surface, as illustrated in Figure 3B.

(29) Widjaja, Y.; Mysinger, M. M.; Musgrave, C. B. *J. Phys. Chem. B* **2000**, *104*, 2527.

(30) Frisch, M. J.; Trucks, G. W.; Schlegel, H. B.; Scuseria, G. E.; Robb, M. A.; Cheeseman, J. R.; Montgomery, J. A., Jr.; Vreven, T.; Kudin, K. N.; Burant, J. C.; Millam, J. M.; Iyengar, S. S.; Tomasi, J.; Barone, V.; Mennucci, B.; Cossi, M.; Scalmani, G.; Rega, N.; Petersson, G. A.; Nakatsuji, H.; Hada, M.; Ehara, M.; Toyota, K.; Fukuda, R.; Hasegawa, J.; Ishida, M.; Nakajima, T.; Honda, Y.; Kitao, O.; Nakai, H.; Klene, M.; Li, X.; Knox, J. E.; Hratchian, H. P.; Cross, J. B.; Bakken, V.; Adamo, C.; Jaramillo, J.; Gomperts, R.; Stratmann, R. E.; Yazyev, O.; Austin, A. J.; Cammi, R.; Pomelli, C.; Ochterski, J. W.; Ayala, P. Y.; Morokuma, K.; Voth, G. A.; Salvador, P.; Dannenberg, J. J.; Zakrzewski, V. G.; Dapprich, S.; Daniels, A. D.; Strain, M. C.; Farkas, O.; Malick, D. K.; Rabuck, A. D.; Raghavachari, K.; Foresman, J. B.; Ortiz, J. V.; Cui, Q.; Baboul, A. G.; Clifford, S.; Cioslowski, J.; Stefanov, B. B.; Liu, G.; Liashenko, A.; Piskorz, P.; Komaromi, I.; Martin, R. L.; Fox, D. J.; Keith, T.; Al-Laham, M. A.; Peng, C. Y.; Nanayakkara, A.; Challacombe, M.; Gill, P. M. W.; Johnson, B.; Chen, W.; Wong, M. W.; Gonzalez, C.; Pople, J. A. *Gaussian 03*, revision B.03; Gaussian, Inc.: Wallingford, CT, 2004.

(31) Note, B3 appears in our exhaustive energetics calculations[22] but is not discussed in the present paper.

(32) Smedarchina, Z. K.; Zgierski, M. Z. *Int. J. Mol. Sci.* **2003**, *4*, 445.

(33) Pilling, M. J.; Seakins, P. W. *Reaction Kinetics*; Oxford Science Publications: Oxford, 1995.

(34) Hill, E.; Freelon, B.; Ganz, E. *Phys. Rev. B* **1999**, *60*, 15896.